

RESEARCH ARTICLE

AtHKT1 drives adaptation of *Arabidopsis thaliana* to salinity by reducing floral sodium content

Dong An^{1,2}, Jiu-Geng Chen¹, Yi-Qun Gao^{1,3}, Xiang Li¹, Zhen-Fei Chao^{1,4}, Zi-Ru Chen^{1,3}, Qian-Qian Li^{1,3}, Mei-Ling Han¹, Ya-Ling Wang¹, Yong-Fei Wang¹, Dai-Yin Chao^{1*}

1 National Key Laboratory of Plant Molecular Genetics, Chinese Academy of Sciences Center for Excellence in Molecular Plant Sciences, Institute of Plant Physiology and Ecology, Chinese Academy of Sciences, Shanghai, China, **2** College of Agriculture and Biology, Shanghai Jiao Tong University (SJTU), Shanghai, China, **3** University of Chinese Academy of Sciences, Beijing, China, **4** Institute of Plant Stress Biology, State Key Laboratory of Cotton Biology, Department of Biology, Henan University, Kaifeng, China

* dychao@sibs.ac.cn



OPEN ACCESS

Citation: An D, Chen J-G, Gao Y-Q, Li X, Chao Z-F, Chen Z-R, et al. (2017) *AtHKT1* drives adaptation of *Arabidopsis thaliana* to salinity by reducing floral sodium content. PLoS Genet 13(10): e1007086. <https://doi.org/10.1371/journal.pgen.1007086>

Editor: Justin O. Borevitz, The Australian National University, AUSTRALIA

Received: August 3, 2017

Accepted: October 20, 2017

Published: October 30, 2017

Copyright: © 2017 An et al. This is an open access article distributed under the terms of the [Creative Commons Attribution License](https://creativecommons.org/licenses/by/4.0/), which permits unrestricted use, distribution, and reproduction in any medium, provided the original author and source are credited.

Data Availability Statement: All relevant data are within the paper and its Supporting Information files

Funding: This study was funded by the Natural Science Foundation of China (<http://www.nsf.gov.cn/>, 31422007 to DYC and 31500994 to DA), Chinese Thousand Talents Program grant (<http://www.1000plan.org/>, to DYC) Chinese Academy of Sciences (<http://www.cas.cn/>, XDPB0402 to DYC) and National Key Laboratory of Plant Molecular Genetics (<http://www.nlpmg.ac.cn/>, to DYC). The funders had no role in study design, data collection

Abstract

Arabidopsis thaliana high-affinity potassium transporter 1 (*AtHKT1*) limits the root-to-shoot sodium transportation and is believed to be essential for salt tolerance in *A. thaliana*. Nevertheless, natural accessions with ‘weak allele’ of *AtHKT1*, e.g. Tsu-1, are mainly distributed in saline areas and are more tolerant to salinity. These findings challenge the role of *AtHKT1* in salt tolerance and call into question the involvement of *AtHKT1* in salinity adaptation in *A. thaliana*. Here, we report that *AtHKT1* indeed drives natural variation in the salt tolerance of *A. thaliana* and the coastal *AtHKT1*, so-called weak allele, is actually hyper-functional in reducing flowers sodium content upon salt stress. Our data showed that *AtHKT1* positively contributes to saline adaptation in a linear manner. Forward and reverse genetics analysis established that the single *AtHKT1* locus is responsible for the variation in the salinity adaptation between Col-0 and Tsu-1. Reciprocal grafting experiments revealed that shoot *AtHKT1* determines the salt tolerance of Tsu-1, whereas root *AtHKT1* primarily drives the salt tolerance of Col-0. Furthermore, evidence indicated that Tsu-1 *AtHKT1* is highly expressed in stems and is more effective compared to Col-0 *AtHKT1* at limiting sodium flow to the flowers. Such efficient retrieval of sodium to the reproductive organ endows Tsu-1 with stronger fertility compared to Col-0 upon salt stress, thus improving Tsu-1 adaptation to a coastal environment. To conclude, our data not only confirm the role of *AtHKT1* in saline adaptation, but also sheds light on our understanding of the salt tolerance mechanisms in plants.

Author summary

Identifying the genetic variation driving plant adaptation to salinity is critical for understanding natural selection and evolutionary mechanisms. In this study, we have revealed that the gene *AtHKT1* drives natural variation in the adaptation of *A. thaliana* to salinity.

and analysis, decision to publish, or preparation of the manuscript.

Competing interests: The authors have declared that no competing interests exist.

Our evidences directly show that the *AtHKT1* allele in the coastal accession Tsu-1 endows *A. thaliana* with enhanced adaptability to salinity. Our further experiments have demonstrated that the enhanced adaptability of the coastal accession is attributed to high *AtHKT1* expression in stems, leading to low sodium levels in flowers. Our work not only elucidates the role of *AtHKT1* in local adaptation to salinity but also improves our understanding of salt tolerance mechanisms of plants.

Introduction

Although plants are sessile and are passively exposed to varying environments, they can successfully complete their life cycle and disperse across a range of environmental conditions. These capabilities are attributable to their physiological plastic and complex gene regulation networks, as well as to their affluent genetic diversities. Therefore, revealing the genetic variation that drives adaptation to particular environments is critical for understanding natural selection and evolutionary mechanisms. Numerous studies have elucidated the genetic changes in different plant species in their adaptation to extreme temperature [1], flowering time [2], photoperiod [3], and microbial attack [4]. Soil is a key environmental factor in maintaining plant growth and a major driving force in plant evolution. Nevertheless, little progress has been made in determining the genetic basis underlying plant adaptation to different edaphic conditions.

Sodium is a non-essential element that is toxic to most plants. Saline soil is an important driver of genetic variation. A previous study has shown that genome duplication alters fitness to allow plants to adapt to saline environments [5]. Nonetheless, only very limited evidence supports the involvement of a specific gene in local adaptation to saline habitats.

HKT1 (*High-affinity Potassium Transporter*) was first isolated from wheat and was shown to function as a K^+/Na^+ symporter [6]. Its homologs in various species, such as *AtHKT1*, *OsHKT1;1* and *SKC1/OsHKT1;5*, are generally expressed in xylems of different organs and contribute to plant salt tolerance by unloading sodium from the transpiration stream [7–11]. Interestingly, natural variation in these *HKT* homologs has been observed in both *A. thaliana* and rice populations. Four amino acid substitutions in *SKC1/OsHKT1;5* significantly increase its sodium transport activity, restricting sodium flux to leaves and greatly enhancing the salt tolerance of the salt-tolerant rice variety Nona Bokra [9].

A. thaliana is widely distributed in all kinds of geographical environments, and many ecotypes have adapted to saline conditions [12]. Tsu-1 and Ts-1 are two coastal *A. thaliana* accessions that are highly tolerant to salt stress [13]. However, unlike the salt-tolerant rice variety Nona Bokra, they accumulate very high sodium in their leaves. Genetic analysis has revealed that the high leaf sodium phenotypes of Tsu-1 and Ts-1 are controlled by the *AtHKT1* locus [13]. *AtHKT1* is expressed at extremely low levels in the roots of these two accessions due to the absence of a distal enhancer [14]. Genome-wide association studies (GWAS) have confirmed that *AtHKT1* controls the natural variation of leaf sodium content in *A. thaliana* populations worldwide and have revealed that *A. thaliana* accessions with weak *AtHKT1* alleles are predominantly distributed in coastal or saline areas [15]. These results, together with other molecular ecology evidence, suggest that *AtHKT1* plays a negative role in the salinity adaptation of *A. thaliana* [12]. However, this conclusion seemingly conflicts with the observation that the null *hkt1-1* mutant is hypersensitive to salt stress [16–18]. Solving this puzzle is particularly important because it may uncover the role of *AtHKT1* in local adaptation, improve our

knowledge of the salt tolerance mechanisms of plants and help resolve the long debate about the relationship between shoot sodium content and salt tolerance.

Edaphic salinity threatens plants via osmotic stress and ion toxicity. Halophyte plants generally accumulate sodium in their shoots, as high sodium helps cells resist osmotic stress, and the sodium is not toxic to the cell as long as it is sequestered in the vacuole [19]. Although *A. thaliana* is not a halophyte, the low expression of *AtHKT1* and the high leaf sodium phenotype of coastal salt-tolerant accessions might suggest that *A. thaliana* may use a strategy similar to halophytes to adapt to saline habitats. It was therefore hypothesized that *AtHKT1* might serve as a double-edged sword for salt tolerance, while weak expression of *AtHKT1* could well balance the osmotic and ionic toxicity of high salt for the best salt tolerance [13,15]. Alternatively, *AtHKT1* might contribute to saline adaptation in an uncharacterized mechanism. Otherwise, it should be independent of the saline adaptation.

Seed production is a key index used for evaluating crops economic efficiency in agriculture and is an essential indicator in assessing the evolutionary adaptation of plants [20]. Therefore, in this study, we used seed yield as a central index for estimating the adaptability of plants. We found that *AtHKT1* positively drives plant adaptation to a coastal environment, by changing its expression pattern to efficiently retrieve sodium from the stem-to-flower xylem sap and thus reduce floral sodium content to increase fecundity upon salt stress.

Results

Salt tolerance of *A. thaliana* has a linear positive relationship with expression levels of *AtHKT1*

To examine if there is an expression balance of *AtHKT1* for the best salt tolerance, independent knockdown lines of *AtHKT1* in the Col-0 background were established. We also isolated an *athkt1* null mutant in the Col-0 background as a positive control by backcrossing *hkt1-1* with Col-0. Under normal condition, no difference on fecundity was observed among different genotypes (Fig 1A and 1B). Though the coastal saline-adapted accession Tsu-1 produced twice as many seeds as Col-0, whereas the *athkt1* knockout mutant yielded almost no seeds when they were treated with 100 mM NaCl, a mild salt stress condition that mimics the natural saline habitat of coastal *A. thaliana* accessions (Fig 1A and 1C). These data indicate that *AtHKT1* is essential for salt tolerance and that Tsu-1 is more adapted to saline soil. Moreover, the number of seeds in *AtHKT1* knockdown lines declined with decreases in *AtHKT1* levels, while those expressing *AtHKT1* to a similar level as Tsu-1 produced a similar number of seeds as *athkt1* (Fig 1A, 1C and 1D). In addition, we found that the seed number is positively and linearly correlated with *AtHKT1* expression when exposed to salt stress (Fig 1F), but not under normal condition (Fig 1E). To sum up, these data demonstrate that *AtHKT1* linearly contributes to salt tolerance, and that weak expression of *AtHKT1* does not really balance the osmotic and ionic toxicities for the best salt tolerance.

AtHKT1 is responsible for the saline adaptation phenotype of Tsu-1

A rough mapping has shown that the salt tolerance phenotype of Tsu-1 is linked to the *AtHKT1* locus [13]. Nonetheless, it remained unclear whether *AtHKT1* itself, or a locus linked to *AtHKT1*, controls the phenotype. To address this question, we tried to map the responsible locus or loci by QTL analysis. Epistatic interaction and additive effects generally cause a big problem for mapping QTLs. Fixing genotype of one causal locus could remove or minimize these problems, therefore we synthesized an F₂ population derived from a cross between Tsu-1 and *athkt1*, as both alleles are hypo-functional.

We first examined the productivity of the F1 progeny and observed that F1 plants produced an amount of seeds similar to *Tsu-1* when exposed to 100 mM NaCl (Fig 2A), suggesting that the adaptive trait is probably controlled by one or more dominant loci. An analysis of 201 F2 individuals further confirmed that a single major locus controls saline adaptation, given that the ratio of salt tolerant F2s (153 individuals) and salt sensitive F2s (48 individuals) conforms to 3:1 ($X^2 = 0.08 < X^2_{0.05} = 3.84$) (Fig 2B). To identify the locus, we performed a QTL analysis using 36 polymorphic genetic markers covering all five chromosomes. As expected, we identified a single major QTL on chromosome 4 that contributed to 53.1% of the variance in seed yield under salt stress (Fig 2C). Interestingly, this candidate region contains *AtHKT1*, but none of the NHX genes that could sequester sodium in the vacuole [21].

We employed an enlarged F2 population with 537 individuals and developed 10 polymorphic markers in the candidate region for fine mapping. Based on genotype and phenotype analyses of the F2 individuals or their F3 progenies, we narrowed down the causal gene to a 100-kb region between genetic markers GM635 and GM645 (Fig 2D). This region contains only 26 annotated genes; and only *AtHKT1* is related to salt tolerance (S1 Table), suggesting that the *AtHKT1* is the causal locus for adaptation of *Tsu-1* to saline conditions. To verify this,

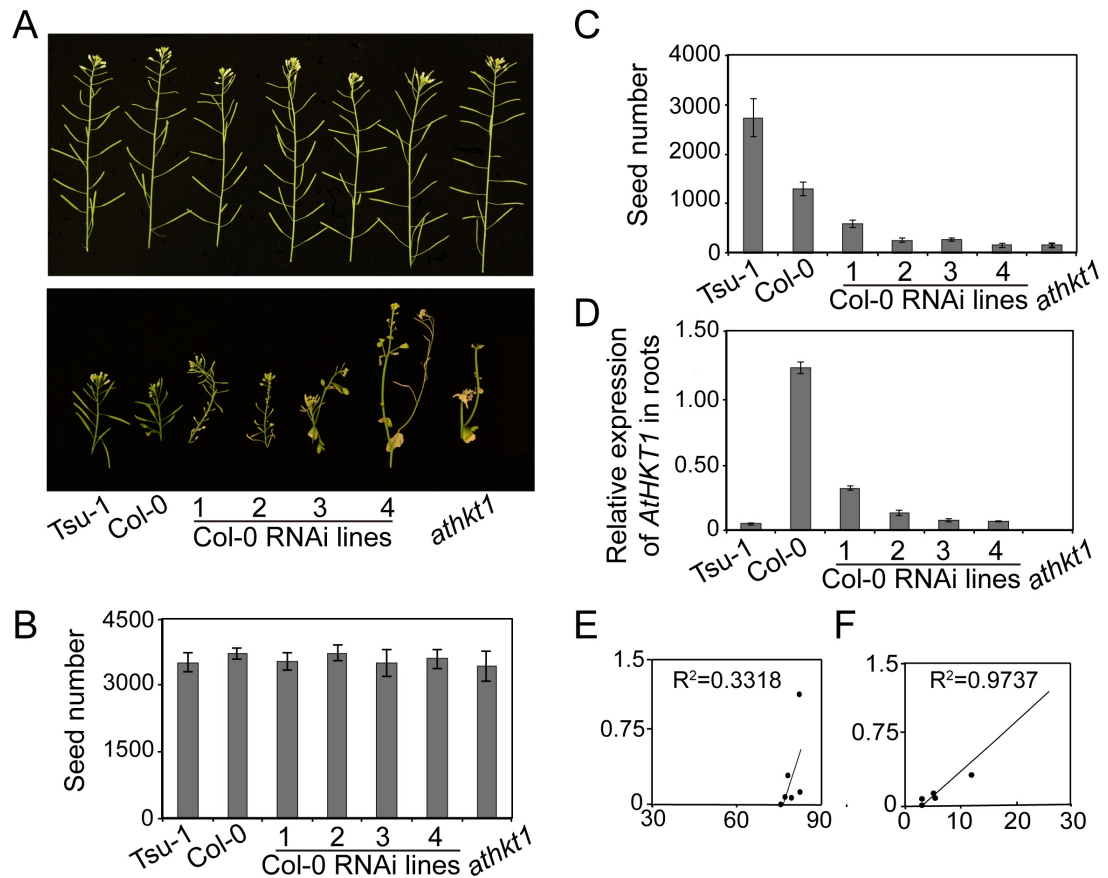


Fig 1. *AtHKT1* contributes to salt tolerance in a linear manner. (A) Flowers and siliques of *Tsu-1*, *Col-0*, *Col-0 AtHKT1* RNAi lines, and *athkt1* under normal conditions (upper) or treated with 100 mM NaCl (lower) for two weeks. (B-C) Numbers of seeds from the plants shown in (A) under normal (B) and 100 mM NaCl treatment conditions (C). Two-week-old plants were treated without or with twice 100 mM NaCl, and seeds were collected continuously during silique maturation. (D) *AtHKT1* expression level assessed by qRT-PCR in the roots of 4-week-old *Tsu-1*, *Col-0*, *Col-0 AtHKT1* RNAi lines, and *athkt1* grown in liquid culture. (E-F) Correlation of seed number and *AtHKT1* expression level under normal (E) and salt stress conditions (F). Data represented with mean \pm SE, $n = 12$, significant differences were determined by ANOVA.

<https://doi.org/10.1371/journal.pgen.1007086.g001>

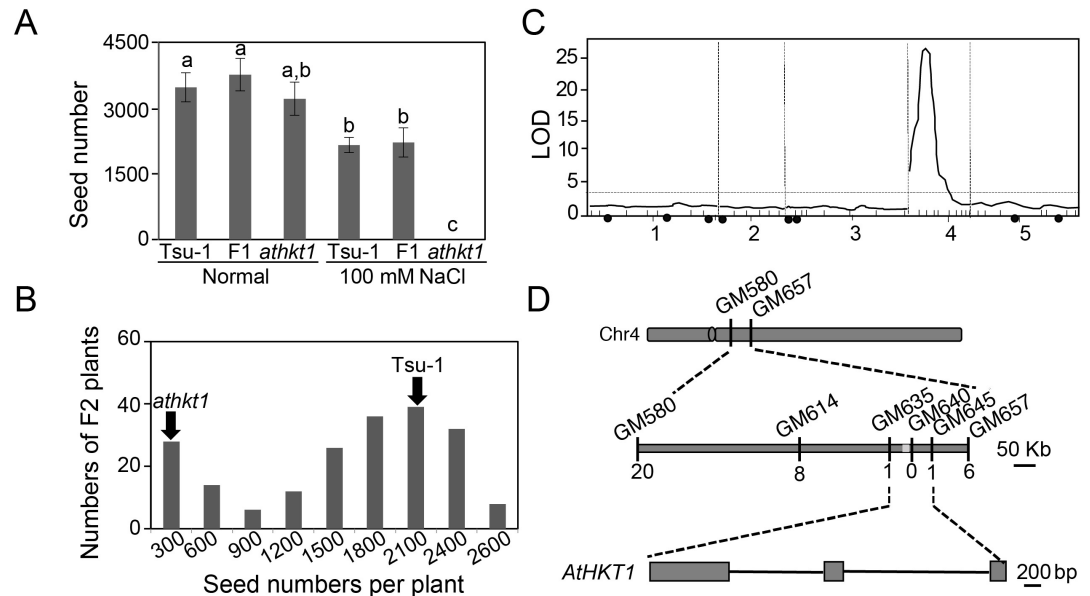


Fig 2. QTL analysis of salt tolerance loci in *Tsu-1* mapped to a single major region where *AtHKT1* is located. (A) Numbers of seeds of F1 plants derived from a cross between *Tsu-1* and *athkt1* under normal and salt stress conditions. Data represented with mean \pm SE, $n = 12$, and significant differences were determined by ANOVA. (B) Numbers of seeds of 201 F2 plants subjected to salt treatment. (C) QTL analysis of the F2 population using the R/qtl package. The threshold of LOD indicated by the dotted line was 2.5. The black dots indicate the genetic locations of 8 NHX genes. (D) Fine mapping of 537 F2 plants using 10 newly developed markers narrowed down the location of the causal gene to a region between GM635 and GM645 on chromosome 4 that contains *AtHKT1*. The number underlined in the middle line indicates recombination events.

<https://doi.org/10.1371/journal.pgen.1007086.g002>

we knocked out *AtHKT1* in *Tsu-1* using CRISPR (clustered regulatory interspaced short palindromic repeats)-Cas9 (CRISPR-associated protein 9) technology [22]. In the T2 generation, we obtained two homologous knockout mutants of *AtHKT1* and named them *hkt1-c1* and *hkt1-c2* (*c* stands for alleles generated by CRISPR-Cas9 technology). In *hkt1-c1*, *AtHKT1* has a thymine inserted between the 450th and 451st nucleotides of the coding sequence (S1A Fig), while, in the *hkt1-c2*, four nucleotides (from the 447th to the 450th nucleotides after the start codon) are deleted (S1B Fig), both of which result in frame shifts.

Under normal conditions, there were no differences on seed production among *hkt1-c1*, *hkt1-c2* and *Tsu-1* (S1C Fig). Yet, when treated with 100 mM NaCl, the two mutants were totally sterile, whereas the wild control *Tsu-1* was still productive (S1D Fig). The phenotypes of the two mutants were comparable to or even more severe than that of *athkt1*, as *athkt1* still produced some seeds, although considerably less than Col-0 under the same conditions (Fig 3A and 3B). Considering that *Tsu-1* produced significantly more seeds than Col-0 in the same salt treatment experiment (Fig 3A and 3B), we conjectured that *AtHKT1* is responsible for the natural variation in saline adaptation between *Tsu-1* and Col-0. To further confirm that the phenotypes of *hkt1-c1* and *hkt1-c2* were caused by *AtHKT1* knock-out, we crossed them with *athkt1* respectively. The F1 plants were all sterile when treated with 100 mM NaCl (S2A and S2B Fig), verifying that the phenotypes of *hkt1-c1* and *hkt1-c2* were not an off-target effect.

To further determine whether a single *AtHKT1* locus is sufficient to drive the variation in the salinity adaptation of *A. thaliana*, we cloned the genomic DNA of *AtHKT1*, including its long promoter from Col-0 and *Tsu-1*, and introduced each construct into the null *athkt1* mutant separately. We tested the salt tolerance of three independent transgenic lines for each construct by assessing productivity. Transgenic lines with either the Col-0 *AtHKT1* fragment

or the *Tsu-1* fragment could complement the salt-hypersensitive phenotype of *athkt1* (Fig 3C). Nevertheless, the Col-0 *AtHKT1* fragment could only restore the saline adaptability of *athkt1* to the Col-0 level, whereas the *Tsu-1* fragment was sufficient to restore *athkt1* to the *Tsu-1* level of adaptability (Fig 3D). These data demonstrated that a single *AtHKT1* locus is sufficient to drive the natural variation in the salinity adaptation of Col-0 and *Tsu-1*.

Reciprocal grafting reveals that the salt tolerance phenotype of *Tsu-1* is driven by shoot *AtHKT1*, whereas that of Col-0 is driven by root *AtHKT1*

Root *AtHKT1* expression drives leaf sodium content in both Col-0 and *Tsu-1* [13]. Nevertheless, it was unclear in what tissue *AtHKT1* drives salt tolerance in these ecotypes. To address this question, we performed two reciprocal grafting experiments; one between *athkt1* and Col-0, and the other was between *hkt1-c1* and *Tsu-1*. We observed that the grafted plants with *athkt1* as the shoot, and Col-0 as the root, were as tolerant as self-grafted Col-0 plants; whereas the grafted plants with Col-0 as the shoot, and *athkt1* as the root, were similar to self-grafted *athkt1* plants (Fig 4A and 4B). This result indicates that salt tolerance of Col-0 predominantly attributes to root *AtHKT1*. However, the grafting experiment between *Tsu-1* and *hkt1-c1* showed the opposite results. The grafted plants with *Tsu-1* scion and *hkt1-c1* stock produced a similar salt tolerant phenotype as *Tsu-1* self-grafted plants, whereas *hkt1-c1* self-grafted plants and grafted plants with *hkt1-c1* scion and *Tsu-1* stock were sterile upon salt stress (Fig 4C and 4D). These data showed that the shoot expression of *AtHKT1* drives the saline adaptation of *Tsu-1*. Moreover, they suggest that although *Tsu-1 AtHKT1* is hypo-functional in roots, it is hyper-functional in shoots.

Tsu-1 AtHKT1 is hyper-functional in stems due to variations in expression

The grafting results inspired us to analyze the expression of *AtHKT1* in different aerial tissues. Quantitative reverse transcription-polymerase chain reaction (qRT-PCR) showed that

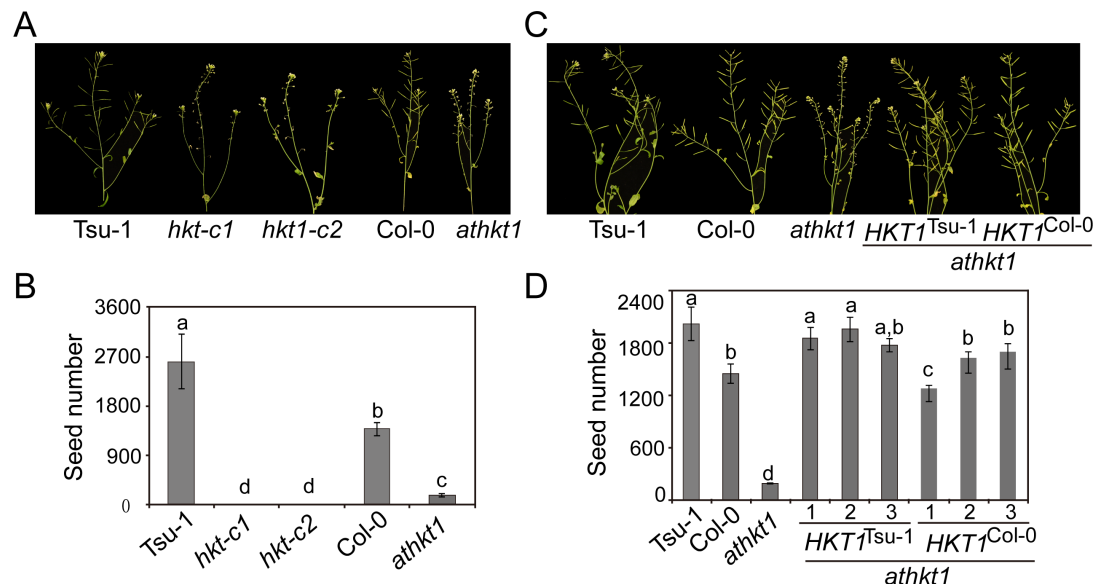


Fig 3. A single *AtHKT1* locus is sufficient to drive natural variation in salinity adaptation. (A) Flowers and siliques of *Tsu-1*, *hkt1-c1*, *hkt1-c2*, Col-0, and *athkt1* subjected to salt treatment. (B) Numbers of seeds of the plants shown in (A) under salt treatment ($n = 12$). (C) Flowers and siliques of *Tsu-1*, Col-0, *athkt1*, and *athkt1* complementation lines with *AtHKT1* fragment from *Tsu-1* or Col-0 following salt treatment. (D) Number of seeds of the plants shown in (C) under salt treatment. ($n > 40$). The plants were treated with 100 mM NaCl twice after growth for 2 weeks. Data represented with mean \pm SE; significant differences were determined by ANOVA.

<https://doi.org/10.1371/journal.pgen.1007086.g003>

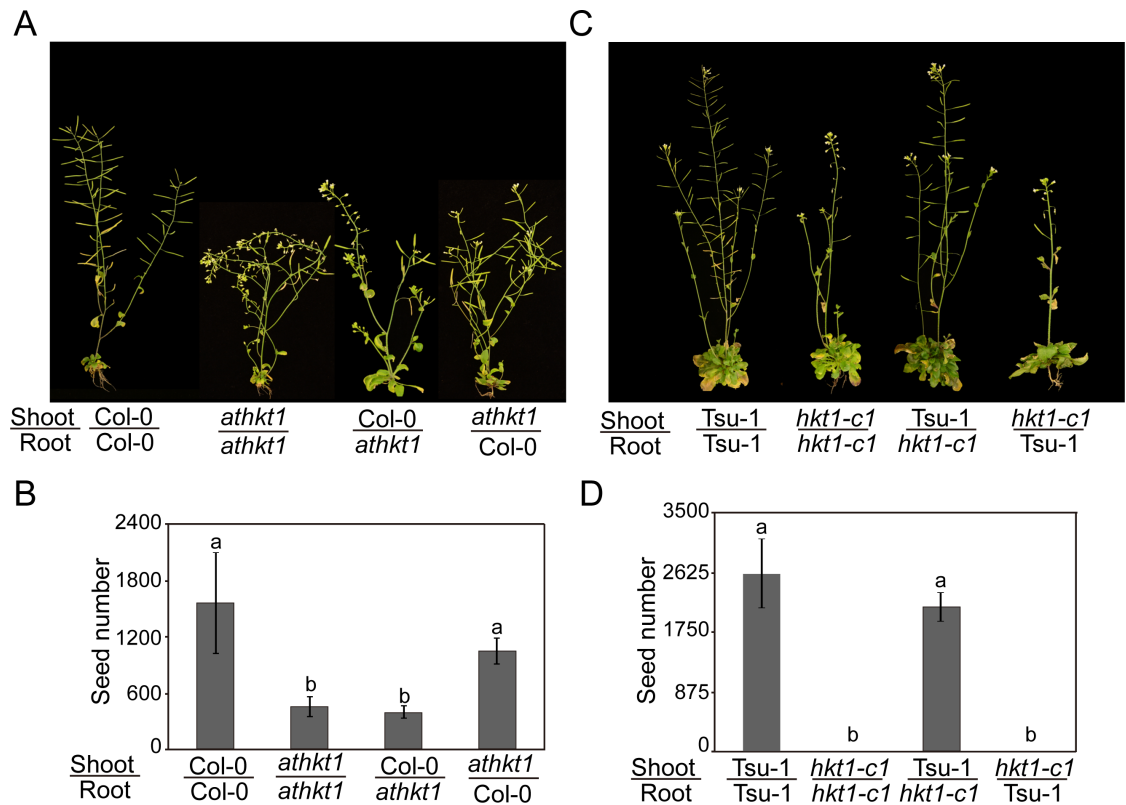


Fig 4. Reciprocal grafting experiments revealed that the salt tolerance phenotype of *Tsu-1* is driven by shoot *AtHKT1*, whereas the phenotype of *Col-0* is driven by root *AtHKT1*. (A) Plants generated via reciprocal graft between *Col-0* and *athkt1* treated with 100 mM NaCl for 2 weeks. (B) Numbers of seeds from reciprocally grafted *Col-0* and *athkt1* plants treated with 100 mM NaCl. (C) Reciprocally grafted plants between *Tsu-1* and *hkt1-c1* subjected to 100 mM NaCl for 2 weeks. (D) Numbers of seeds from reciprocally grafted *Tsu-1* and *hkt1-c1* plants subjected to 100 mM NaCl. Successfully grafted plants ($n > 12$) were transferred to pots for 2 weeks following 100 mM NaCl treatment twice for 2 weeks before images were taken. Data represented with mean \pm SE; significant differences were determined by ANOVA.

<https://doi.org/10.1371/journal.pgen.1007086.g004>

differences in *AtHKT1* expression between *Tsu-1* and *Col-0* depend on the tissue and the treatment. *AtHKT1* was expressed at similar levels in the rosette leaves of 4-week-old of *Tsu-1* and *Col-0* when exposed to 100 mM NaCl for 24 h, but its expression was higher in the rosette leaves of *Col-0* than of *Tsu-1* under normal conditions (S3A Fig). In flowers, *Tsu-1* expressed *AtHKT1* at a similar level as *Col-0* under normal conditions but it expressed less than *Col-0* when treated with salt (S3B Fig). Interestingly, *Tsu-1* expressed significantly higher *AtHKT1* in the stems, cauline leaves and siliques compared to *Col-0* (Fig 5A). When treated with salt, *Tsu-1* expressed 6 times more *AtHKT1* than did *Col-0* in the stems, which is consistent with the hypothesis that *Tsu-1* allele of *AtHKT1* is hyper-functional in shoot.

To confirm the qRT-PCR results and further examine the spatial expression patterns of *AtHKT1* in detail, we generated transgenic *Col-0* plants carrying a β -glucuronidase (GUS) reporter driven by the long promoter of *AtHKT1* from either *Tsu-1* or *Col-0*. We examined 5 independent transgenic lines expressing $pAtHKT1^{Tsu-1}::GUS$ and 7 independent lines expressing $pAtHKT1^{Col-0}::GUS$. The transgenic lines containing the same construct showed consistent GUS signals. At the seedling stage, all 5 lines expressing $pAtHKT1^{Tsu-1}::GUS$ exhibited very weak GUS activity in the roots, whereas 6 of the 7 lines expressing $pAtHKT1^{Col-0}::GUS$ strongly expressed GUS in the stele of the roots (Fig 5B). These observations were consistent with previous findings [14] and with our qRT-PCR results (Fig 5C), indicating that the constructs were

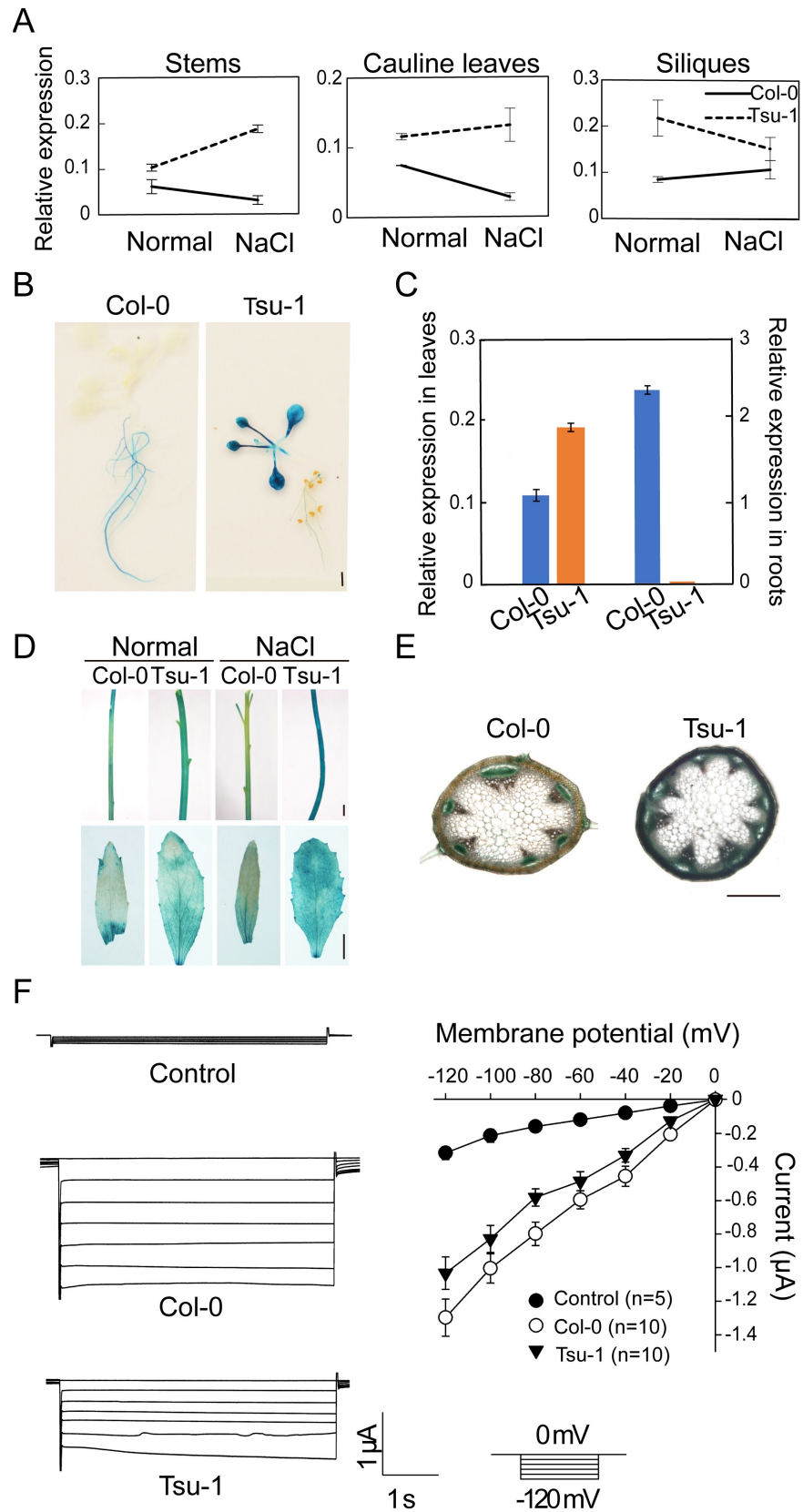


Fig 5. *AtHKT1* is hyper-functional in *Tsu-1* stems. (A) *AtHKT1* expression in the stems, cauline leaves, and siliques of 4-week-old *Tsu-1* and *Col-0* before and after 100 mM NaCl treated for 24 h. Data represented with mean \pm SE, $n = 6$. (B) GUS staining of 2-week-old T1 transgenic seedlings expressing *pAtHKT1:GUS* from *Col-0* and *Tsu-1*. (Scale bar: 0.5 cm). (C) *AtHKT1* expression in the shoots and roots of *Tsu-1* and *Col-0*. Two-week-old seedlings grown on 1/2 MS medium. (D) GUS staining of the stems and cauline leaves of transgenic lines expressing *pAtHKT1:GUS* from *Col-0* and *Tsu-1*. Four-week-old transgenic plants grown in pots before (Normal) and after 100 mM NaCl treatment for 24 h (NaCl). (Scale bars: 0.5 cm). (E) GUS staining of the stems of 4-week-old transgenic lines expressing *pAtHKT1:GUS* from *Col-0* (upper) and *Tsu-1* (lower) by hand sectioning. (Scale bar: 250 μ m). (F) Electrophysiological recording of the activity of *AtHKT1* from *Tsu-1* and *Col-0*. The current-voltage curves were measured using a ramp command in which the membrane potential was stepped from -120 mV to 0 mV. The data shown here are the steady-state current-voltage curve (mean \pm SE) in the bath solution containing 10 mM Na⁺ and 0.3 mM K⁺.

<https://doi.org/10.1371/journal.pgen.1007086.g005>

correctly expressed in *Col-0* plants. Contrary to the root results, the GUS signal in stems and cauline leaves of 4-week-old of plants was much stronger in *Tsu-1* than in *Col-0* (Fig 5D). This result further confirmed the qRT-PCR results.

We further examined the detailed expression site(s) of *AtHKT1* in stems by hand sectioning of the *pAtHKT1:GUS* transgenic lines. The GUS signal driven by the *Tsu-1 AtHKT1* promoter was mainly observed in the xylem of the stem (Fig 5E), indicating that *Tsu-1 AtHKT1* predominantly functions in removing sodium from the flux to the flowers. By contrast, the GUS signal driven by *Col-0 AtHKT1* promoter was very weak in the xylem and was observable in the phloem (Fig 5E). These data demonstrated that variation in the *AtHKT1* promoter affects not only the expression level but also the spatial specificity of *AtHKT1* expression.

In addition to large insertion/deletion (indel) polymorphisms in the promoter region (S4A Fig), multiple single nucleotide polymorphisms (SNPs) were also observed in the coding sequence with several affecting the amino acid sequence (S4B Fig). To test whether the amino acid changes in *AtHKT1* in *Tsu-1* affect its transport activity, we expressed *AtHKT1* protein from *Tsu-1* and *Col-0* in *Xenopus laevis* oocytes for electrophysiological analysis. As expected, we detected sodium transporter activity of *AtHKT1* (Fig 5F), but there was no significant difference between the proteins from *Col-0* and *Tsu-1*, indicating that the amino acid changes do not affect *AtHKT1* activity. This observation is consistent with previous findings that these changed amino acids are not in conserved regions of *AtHKT1* [23,24].

Tsu-1 AtHKT1 is more effective in limiting sodium accumulation in flowers exposed to salt stress

The increased expression of *AtHKT1* in the xylem of *Tsu-1* stems suggested that *Tsu-1* is more effective than *Col-0* at limiting sodium flow to flower. To confirm this hypothesis, we measured the sodium content in the flowers. Under normal conditions, *athkt1* accumulated 38% higher sodium in flowers than *Col-0*, and *hkt1-c1* accumulated 46% higher than *Tsu-1*, but there were no significant differences between the wild-types and between the mutants (Fig 6A). Nevertheless, the sodium content in *Tsu-1* flowers was only 62% of that in *Col-0* flowers when exposed to salt treatment (Fig 6B). By contrast, upon salt stress, the loss of *AtHKT1* function in *Col-0* resulted in a 199% increase in floral sodium, whereas the loss of *AtHKT1* function in *Tsu-1* resulted in a 275% increase in floral sodium (Fig 6B). These data indicated that *AtHKT1* in *Tsu-1* stems is more effective in limitation of sodium flux to flowers than *AtHKT1* in *Col-0* roots. In addition, we analyzed the relationship between floral sodium content and seed number under salt stress and found these two variables to be negatively correlated (Fig 6B Embedded), demonstrating that the sodium content in flowers under salt stress is a determinant of saline adaptation.

An examination of stem sodium content provided additional evidence supporting the idea that *Tsu-1 AtHKT1* is involved in sodium removal in stems. There was no significant

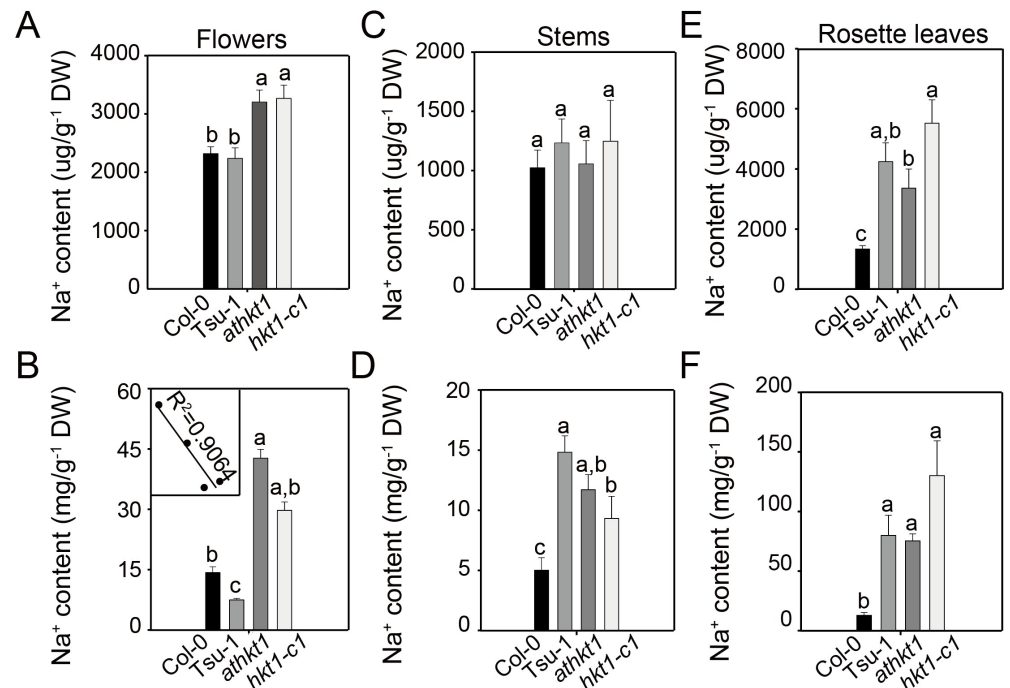


Fig 6. Na⁺ content of Col-0, Tsu-1, *athkt1* and *hkt1-c1*. (A) Na⁺ content in flowers under normal conditions. (B) Na⁺ content in flowers under salt treatment. Negatively correlated between floral sodium content and seed number under salt stress (*Embedded*) (C) Na⁺ content in stems under normal conditions. (D) Na⁺ content in stems under salt treatment. (E) Na⁺ content in rosette leaves under normal conditions. (F) Na⁺ content in rosette leaves under salt treatment. Five-week-old plants irrigated without or twice with 100 mM NaCl were used to analyze Na⁺ by ICP-MS. Data represented with mean ± SE, n = 12, and significant differences were determined by ANOVA.

<https://doi.org/10.1371/journal.pgen.1007086.g006>

difference in stem sodium content among Col-0, Tsu-1, *athkt1* and *hkt1-c1* under normal conditions (Fig 6C). However, under salt stress, Tsu-1 accumulated 59% more sodium in stems than did *hkt1-c1*, whereas Col-0 accumulated 57% less stem sodium than *athkt1* (Fig 6D); these results show that *AtHKT1* in Tsu-1 promotes sodium accumulation in stems and that *AtHKT1* in Col-0 has the opposite effect. This observation further confirmed that Tsu-1 *AtHKT1* is hyper-functional in restricting sodium flow from stems to flowers and that Col-0 *AtHKT1* functions to limit sodium flow from roots to shoots, and explains why the Tsu-1 allele of *AtHKT1* endows the coastal accessions with higher adaptation ability to salinity environment than the inland accessions.

Previous studies have illustrated that the leaf sodium content cross different *A. thaliana* accessions under normal conditions is not associated with its salinity tolerance [15]. However, the leaf sodium content under salt stress is unknown. Therefore, we also measured the leaf sodium content under normal conditions and after salt treatment. Consistent with previous studies, Tsu-1 and the two null mutants accumulated much more leaf sodium than Col-0 under normal conditions (Fig 6E). The result was similar when the plants were treated with salt, as the leaf sodium content in Tsu-1 and the two null mutants was much higher than that in Col-0 (Fig 6F).

Discussion

The salinization of irrigated land is increasingly detrimental to plant reproduction and agricultural productivity, as most plant species are sensitive to high concentrations of sodium.

Understanding the genetic and molecular mechanisms underlying salt tolerance is necessary for resolving such problems. Natural variation is an important genetic resource for studying gene function, as well as evolutionary biology. Previous studies have shown that HKT family transporters are essential for natural variation in salt tolerance of rice [9,25,26]. *AtHKT1* has also been found to control natural variation in leaf sodium content of *A. thaliana*, but it is still unclear if and how this locus contributes to saline adaptation [13,15]. In this study, we performed a series of experiments to address this question.

AtHKT1 positively contributes to saline adaptation of *A. thaliana*

As seed number is an essential trait for population expansion [20], we used this trait for assessing saline adaptation of plants. Previous studies have suggested that *AtHKT1* might be fine-tuned for balancing the ionic and osmotic stresses caused by high salt, as weak alleles of *AtHKT1* might improve salt tolerance, whereas null alleles of *AtHKT1* suppress salt tolerance [13]. Our observation of the linear relationship between salt tolerance and *AtHKT1* expression levels argued against this hypothesis. However, our QTL analysis suggested that *AtHKT1*, but not additional locus, control the salt adaptability of Tsu-1. Knockout of *AtHKT1* in Tsu-1 by CRISPR-Cas9 technology and complementation *athkt1-1* with Tsu-1 and Col-0 *AtHKT1* finally established that *AtHKT1* is not only a requirement for salt tolerance of Tsu-1 but is also a predominant, if not sole locus that drives the natural variation in salinity adaptation between Col-0 and Tsu-1. Though *AtHKT1* has been found to drive natural variation in leaf sodium content, this is the first direct evidence to show that *AtHKT1* plays a positive role in natural selection of saline adaptive *A. thaliana* accessions. These genetic evidences revealed that the Tsu-1 allele of *AtHKT1* is hyper-functional but not hypo-functional.

The saline adaptive accession Tsu-1 employs a more efficient mechanism of *AtHKT1* for restricting sodium accumulation in flowers

Our grafting experiments revealed that the saline adaptability of Tsu-1 is driven by shoot *AtHKT1* expression, which is in contrast with the premise that salt tolerance of Col-0 is predominantly driven by root *AtHKT1* expression. This data indicates that *AtHKT1* functions differently in different accessions. GUS reporter system and qRT-PCR confirmed that Tsu-1 *AtHKT1* is hyper-functional relative to Col-0 *AtHKT1* due to its high expression in stems. Interestingly, histochemical staining experiment revealed that Tsu-1 *AtHKT1* is predominantly expressed in xylem parenchyma cells of stems, suggesting that it functions in restricting sodium in the stems. Measurements of stem and floral sodium concentrations of different genotypes confirmed this hypothesis. Therefore, the Tsu-1 *AtHKT1* functions through a new mechanism, which is to restrict sodium in the leaves and stems. This mechanism is in contrast with that of Col-0 *AtHKT1* that restricts sodium in the roots.

Flower is the most important organ of the plant. However, the germ cells in flowers are very sensitive to sodium, as such cells are weak in sodium compartmentalization and detoxification due to low vacuole capacity. By contrast, leaf cells have very large vacuoles; thus, even if they accumulate a high level of sodium, it is not highly toxic if it is sequestered in the vacuole [19]. Instead, the high accumulation of sodium in leaves would facilitate resistance to osmotic stress. This difference results in flowers being much more sensitive to salt compared to leaves. Consequently, reducing the flower sodium content but not the leaf or stem sodium content is much more important for *A. thaliana* upon salt stress. The Tsu-1 *AtHKT1* and the Col-0 *AtHKT1* represent two mechanisms for restricting sodium flow to flowers; Tsu-1 *AtHKT1* unloads sodium to the leaves and stems, and Col-0 unloads sodium in the roots. According to the floral sodium concentrations in Tsu-1 and Col-0, we can conclude that the Tsu-1 mechanism is

more effective than Col-0 mechanism in limiting sodium flow to flowers. In addition, a previous study has shown that the Col-0 mechanism could inhibit root growth upon salt stress due to its improving sodium accumulation in the roots [17]. These findings together explain why the mechanism of Tsu-1 *AtHKT1* endows *A. thaliana* with a higher adaptation ability to saline conditions.

However, we also noticed that the Col-0 mechanism was selected by most inland accessions though it represents a low efficient mechanism in salt tolerance. So far, it is hard to conclude what is the driving force behind the selection of such a mechanism, but we suspect that it might be associated with the edaphic sodium concentrations. Inland soil contains subtoxic levels of sodium, and accumulating sodium in the roots thus might be the most economical way for *A. thaliana* to minimize the side-effect of sodium on flower development. By contrast, the Tsu-1 mechanism involves transporting of sodium to shoot cells and sequestering it into the vacuoles that consume much more energy. Therefore, the selection of Col-0 mechanism or Tsu-1 mechanism might reflect the sodium levels in their habitat.

The polymorphisms in the promoter region might be responsible for the divergence in expression between Col-0 *AtHKT1* and Tsu-1 *AtHKT1*

According to a previous study, one of the tandem repeats in the distal promoter of *AtHKT1* is an enhancer that promotes the expression of *AtHKT1* in roots, and the absence of this distal repeat in Tsu-1 was confirmed to be responsible for the down regulation of *AtHKT1* in roots [13]. However, we noted in the results of a previous study that the expression of *AtHKT1* is apparently upregulated in shoots and markedly downregulated in roots in the absence of this hypothesized distal enhancer [14]. In our study, the expression of Tsu-1 *AtHKT1* was significantly higher than that of Col-0 *AtHKT1* in the shoots of young seedlings. This observation suggested that the second tandem repeat might not only serve as an enhancer in roots but may also function as a repressor in shoots. In this case, the high expression of *AtHKT1* in Tsu-1 stems is probably caused by the deletion of the second tandem repeat. *AtHKT1* has also been reported to be regulated by DNA methylation in the promoter [14]. However, we found no difference of the small RNA target site in the promoters of *AtHKT1* between Tsu-1 and Col-0 (S4 Fig). Of course, we cannot exclude the possibility that other polymorphisms among the many in the promoter region control the variation in *AtHKT1* expression patterns. Further research is necessary to clarify this question.

Floral sodium contents upon mild salt stress might be a better indicator of plant adaptation to saline conditions

Shoot sodium content is often used as a parameter for assessing salt tolerance of plants, but the relationship between shoot Na^+ and salt tolerance raises arguments. In rice, low shoot Na^+ is an indicator of salt tolerance [27]. A typical case is the identification of *SKC1/OsHKT1;5* that reduces leaf salt content and enhances salt tolerance [9]. However, it was reported that the growth and yield of wheat upon salt stress is not correlated with sodium concentrations in leaf blade or the whole shoot [28]. Meanwhile, the salt tolerant tomato varieties accumulate higher sodium in stems and leaves than the sensitive varieties [29,30]. These findings suggest that the relationship between shoot sodium content and salt tolerance might be genetic background dependent, and therefore not stable index for assessing plant salt tolerance. This study further supports the above conclusion. In this study, we observed that the sodium levels in flowers, but not in leaves, are positively associated with salinity adaptability. This suggests that floral sodium content might be more suitable for assessing salt tolerance of plants. Of course, this does not mean the leaf sodium does not matter for salt tolerance of plants. Actually, the

increased leaf sodium causes severe leaf necrosis in *athkt1* null mutants when exposed to high salt conditions [16,18,31]. But upon mild salt stress, the flowering phenotype of *athkt1* null mutants is more obvious than the leaf phenotype, as its leaf still has photosynthesis ability (S5A Fig), but it is almost sterile in seed production. Therefore, leaf sodium may play different roles upon different levels of salt conditions. It is worthwhile pointing out that *A. thaliana* is a species of glycophytes and even salt tolerant ecotypes/accessions may not successfully colonize in high salt area. Even Tsu-1 barely produces seeds when exposed to 150 mM NaCl. Therefore, mild salt stress more accurately reflects the real habitat of *A. thaliana*. On the other hand, the leaf necrosis in Tsu-1 caused by high salt treatment is less severe than Col-0 (S5B Fig), though Tsu-1 accumulates as much sodium as *hkt1* null mutants in the leaves. This could be caused by differential expression pattern of *AtHKT1* in leaves, or controlled by some other QTLs/genes.

To our knowledge, the relationship between flower sodium content and saline adaptability has never been reported. Identifying the positive relationship between the two factors provides a new angle to assess plant salt adaptability. Of course, we are not sure if this conclusion could be extended to all plant species in current stage, and further investigation is necessary to answer this question. The seed production is a most important trait of crops in agriculture. Our finding that different expression patterns and levels of *AtHKT1* result in different yield upon salt stress could inspire engineering salt tolerant plants by manipulating expression pattern of *HKT1*. Moreover, this finding could also be translated to crops to improve their yields in saline area.

Materials & methods

Plant material and salt treatment

Seeds of *A. thaliana* were surface sterilized and sown on 1/2 Murashige and Skoog (MS, Sigma-Aldrich, St. Louis, USA) medium (pH 5.7) containing 1% (w/v) sucrose, followed by stratification at 4 °C in dark for 5 days. The seedlings were transferred into pots with artificial soil in a phytotron (16 h light/8 h dark, 22 °C day/20 °C night, 80% humidity, 80 $\mu\text{mol}\cdot\text{m}^{-2}\cdot\text{s}^{-1}$) after being grown on the plates for 7 days. Two-week-old soil-grown plants that were irrigated with 100 mM NaCl twice for two weeks and 1 additional week later plants were used for phenotyping. Four-week-old plants irrigated with 100 mM NaCl for 24 h were used for gene expression analysis and GUS staining. Each line used for salt treatment contained ≥ 12 plants, and every treatment included 3 biological replicates. The *athkt1* mutant was isolated from an F2 population derived from a backcross between *hkt1-1* (CS6531, obtained from the Arabidopsis Biological Resource Center) and Col-0.

Hydroponic culture

Seeds of *A. thaliana* (Tsu-1, Col-0, *AtHKT1* RNAi lines and *athkt1*) were stratified for 5 days at 4 °C in water. The stratified seeds were sowed in punctured holes of 1.5-mL Eppendorf tube caps stuffed with 0.1% agar, and the caps were then placed on 1.5-mL Eppendorf tube containing Hoagland solution for 14 days in a chamber at 22 °C, 70% relative humidity, and light intensity of 80 $\mu\text{mol}\cdot\text{m}^{-2}\cdot\text{s}^{-1}$ on 8 h light/16 h dark. The seedlings together with caps were then transferred to a big box containing Hoagland solution for growing 2 additional weeks. The culture solution was refreshed every 5 days. The roots of one-month-old seedlings were collected for qRT analysis.

QTL mapping analysis

An F2 population derived from Tsu-1 and *athkt1* was used to map the causal gene of the salt tolerance of Tsu-1. The number of seeds was calculated based on an estimation of the total

grain weight and 100-grain weight. A set of 36 CAPS (Cleaved Amplified Polymorphism Sequences) and SSR (Simple Sequence Repeat) markers covering the 5 chromosomes of *A. thaliana* were used to genotype all F2 individuals. QTL analysis was performed using the R/qtI package (<http://www.rqtI.org>). To narrow down the candidate region, 537 F2 individuals and 10 newly developed CAPS markers were used to fine map the target region. All CAPS and SSR markers are listed in [S2 Table](#).

Vector construction and plant transformation

For the complementation experiment, a 9.3-kb *AtHKT1* fragment including a 5.3-kb promoter region from Col-0 was amplified by overlap PCR using primers HKT-pro-gene L, PHMS-HKT1-MID-R, PHMS-HKT1-MID-L and HKT-pro-gene R ([S3 Table](#)). The complementation fragment for Tsu-1 *AtHKT1* was amplified using the same strategy but with primers Tsu-HKT-pro-gene L, PHMS-HKT1-MID-R, PHMS-HKT1-MID-L and HKT-pro-gene R. The fragments were cloned into a binary vector, pHMS, which was modified from the pHB vector [32] by infusion recombination cloning using a Hieff Clone One-step PCR Cloning Kit (Yisheng Co. Ltm, Shanghai, China).

To construct the *promoter:GUS* vector, the *AtHKT1* promoters were amplified from genomic DNA using primers HKT-GUSL TONG and HKT-GUSR TONG for Col-0 and primers HKT-GUSL TONG 2 and HKT-GUSR TONG for Tsu-1. The fragments were recombined into the binary vector pCAMBIA1303 using the Hieff Clone One-step PCR Cloning Kit. GUS histochemical staining was performed as described previously [9].

To construct the Col-0 *AtHKT1* RNAi vector, two 184-bp fragments from the *AtHKT1* full-length cDNA sequence were amplified using the primers *AtHKT1 F* (*Pst*I restriction site) and R (*Xba*I restriction site) for sense and *AtHKT1 F* (*Sac*I restriction site) and R (*Not*I restriction site) for antisense. Both amplified fragments were sequenced and inserted into an intermediate vector, pBluescript II SK (+/-), containing a 120-nucleotide intron from the *A. thaliana* RTM1 gene at the *Xba*I and *Not*I sites. Then, the hairpin fragment was sub-cloned into the binary vector pCAMBIA2301, which contained a cauliflower mosaic virus (CaMV) 35S promoter and a NOS terminator. The kanamycin resistance gene (*NPT II*) was used as a selective marker gene.

The construction of a CRISPR-Cas9 vector targeting *AtHKT1* was performed as described previously [22]. Two oligos, *AtHKT1* sgRNA4-F and sgRNA4-R, were synthesized and annealed to form a target site of 20bp in length with a requisite proto-spacer-adjacent motif, PAM (NGG) sequence at the 3' end and G at the 5' end of the sequence. The target site, containing two *Bbs*I digestion sites, was cloned into the intermediate vector AtU6-26SK. The chimeric RNA expression cassette between *Kpn*I and *Sal*I was cloned into the *Kpn*I and *Eco*RI sites of the pCambia1300 vector (Cambia, Canberra, Australia) together with the *Sal*I and *Eco*RI fragment of the Cas9 expression cassette from the 35S-Cas9-SK vector, which was a gift from the Zhu lab [22].

The expression constructs were transformed into *Agrobacterium tumefaciens* strain GV3101, and were then introduced into the backgrounds as indicated using the floral dip method (26). Transgenic lines were screened on 1/2 MS medium solidified with agar containing 50 mg/L hygromycin and 1% sucrose.

Electrophysiological analysis of AtHKT1 in *X. laevis* oocytes

We inserted the cDNA of *AtHKT1* from the Col-0 and Tsu-1 alleles into the *Sma*I site of the expression vector pGEMHE. The capped cRNA was transcribed using the RiboMAX Large Scale RNA Production System-T7 kit (P1300, Promega, Wisconsin, USA). The cRNA quality was verified using agarose gel electrophoresis. The concentration was determined at 260 and

280 nm and adjusted to a final concentration of $0.8 \mu\text{g} \mu\text{l}^{-1}$. We injected freshly isolated *X. laevis* oocytes with 23 nL of cRNA and used the oocytes for voltage-clamp experiments 3–4 days later. Electrophysiological experiments were conducted using a two-electrode voltage clamp amplifier as described previously [9]. We bathed the oocytes in a solution containing 6 mM MgCl_2 , 1.8 mM CaCl_2 , 10 mM MES-Tris (pH 5.5), 185 mM D-mannitol and 10 mM Na-glutamate salts. The voltage protocols used are described in the figure legends.

ICP-MS analysis

The process of *A. thaliana* elemental analysis via inductively coupled plasma mass spectrometry (ICP-MS) has been described previously [33]. Briefly, different tissues, including flowers, whole stems and rosette leaves, from five-week-old plants treated twice with 100 mM NaCl or from untreated plants were cut with a scalpel while holding the plants with plastic tweezers. The collected tissues were rinsed with four times with 18-M Ω water in a 1000-mL breaker to wash off the impurities. Then, the rinsed samples were placed into a glass tube, and the samples were shifted to the bottom of the tube, making sure that no samples were left on the tube wall. The tubes were transferred to an oven at 65°C for 12 h. After cooling, twelve samples were weighed out on an analytical balance. All the samples, including the blank controls, were digested with 1 mL of concentrated nitric acid containing an indium (In) internal standard at 115°C for 4 h, and then the digested samples were diluted to 10 mL with 18 M Ω water. Elemental analysis for Li, B, Na, Mg, P, S, K, Ca, Mn, Fe, Co, Ni, Cu, Zn, As, Se, Rb, Sr, Mo, and Cd was performed using an ICP-MS (NexION 350D; PerkinElmer) coupled to an Apex desolvation system and an SC-4 DX auto sampler (Elemental Scientific Inc., Omaha, NE, US). All samples were normalized to calculate weight, as determined using a heuristic algorithm using the best-measured elements, the weights of the eight weighed samples, and the solution concentrations, as previously described.

Grafting of *A. thaliana* plants

Seedlings were grafted as previously described [13]. Graft unions were examined under a stereoscope before transfer to potting soil to identify any adventitious root formation at or above the graft unions. Healthy grafted plants were transferred to pots and grown in a controlled environment for 2 weeks. Then, the plants were irrigated with a 100 mM NaCl solution twice, and after 2 weeks, the plants were photographed. After harvesting, the graft unions were examined again, and grafted plants with adventitious roots or without a clear graft union were excluded from subsequent analysis.

qRT-PCR

Total RNA was extracted from plants using TRNzol A+ RNA Purification reagent (TIANGEN, DP421, Beijing, China). Two micrograms of total RNA were used to synthesize first-strand cDNA with TransScript One-Step gDNA Removal and cDNA Synthesis SuperMix (Transgen, AT311-02, Beijing, China). qRT-PCR was performed using SYBR Green PCR Master Mix (TRT-101, TOYOBO, Osaka, Japan) with the first-strand cDNA as a template on a Real-Time PCR System (Bio-Rad CFX thermocycler, California, USA). Primers for qRT-PCR were designed using Primer Express Software Version 3.0 (Applied Biosystems, USA). The primers HKT1 exon2-3-1L and HKT1 exon2-3-1R were designed to span an exon-exon junction and were used to detect the gene expression level. The primers UBCF and UBCR were designed for *UBIQUITIN-CONJUGATING ENZYME21* (At5g25760), which was used as the control gene. The primer sequences are shown in S3 Table. Expression data analysis was performed as described previously [34].

Supporting information

S1 Fig. Targeted indel mutations induced by engineered sgRNA:Cas9 at the *AtHKT1* gene in *Tsu-1*. (A) A thymine insertion between the 450th and 451st nucleotides of *AtHKT1* coding sequence. (B) Four-nucleotide deletion between the 447th and 450th of *AtHKT1* coding sequence shown in red box. Sequences shown were amplified from genomic DNA and sequenced after cloned into vectors. (C) Phenotypes of *Tsu-1*, *hkt1-c1* and *hkt1-c2* under normal conditions. (D) Phenotypes of *Tsu-1*, *hkt1-c1* and *hkt1-c2* under salt stress condition. Five-week-old plants irrigated without or twice with 100 mM NaCl were taken photographed. (TIFF)

S2 Fig. Allelism test of *hkt1-c1*, *hkt1-c2* and *athkt1*. (A) F1 plants derived from a cross between *athkt1* and *hkt1-c1* under salt stress condition. (B) F1 plants derived from a cross between *athkt1* and *hkt1-c2* under salt stress condition. Five-week-old plants were irrigated twice with 100 mM NaCl. (TIFF)

S3 Fig. Expression of *AtHKT1* in rosette leaves (A) and flowers (B) in *Col-0* and *Tsu-1* revealed by qRT-PCR. Four-week-old plants before and after treatment with 100 mM NaCl for 24 h. Data represented with mean \pm SE, $n = 6$. (TIFF)

S4 Fig. Polymorphisms of *AtHKT1* between *Col-0* and *Tsu-1*. (A) Major large indel polymorphisms of *AtHKT1* between *Col-0* and *Tsu-1*. (B) Detailed polymorphisms of *Tsu-1 AtHKT1* compared to *Col-0 AtHKT1*. (TIFF)

S5 Fig. Photosynthetic changes of *Col-0*, *athkt1* and *Tsu-1* when exposed to salt stress. Four-week-old plants before and after treatment with 100 mM NaCl for 3 days. Fv/Fm, an indicator for light-adapted maximum quantum yield of PSII, was measured at 0 day, 1 day, 2 day and 3 day post-salt treatment. (TIFF)

S1 Table. List of genes in the 100-kb candidate region between genetic markers GM635 and GM645. (DOCX)

S2 Table. Primers used for QTL mapping. (DOCX)

S3 Table. Primers used for sequencing and vector construction. (DOCX)

Acknowledgments

We thank Prof. Jian-Kang Zhu for kindly providing us the CRISPR-Cas9 vectors.

Author Contributions

Conceptualization: Dai-Yin Chao.

Data curation: Dong An.

Formal analysis: Dong An.

Funding acquisition: Dai-Yin Chao.

Investigation: Dong An, Jiu-Geng Chen, Yi-Qun Gao, Xiang Li, Zhen-Fei Chao, Zi-Ru Chen, Qian-Qian Li, Mei-Ling Han, Ya-Ling Wang.

Project administration: Dai-Yin Chao.

Supervision: Yong-Fei Wang, Dai-Yin Chao.

Writing – original draft: Dong An, Dai-Yin Chao.

References

1. Ma Y, Dai X, Xu Y, Luo W, Zheng X, Zeng D, et al. *COLD1* confers chilling tolerance in rice. *Cell*. 2015; 160: 1209–1221. <https://doi.org/10.1016/j.cell.2015.01.046> PMID: 25728666
2. Li Y, Huang Y, Bergelson J, Nordborg M, Borevitz JO. Association mapping of local climate-sensitive quantitative trait loci in *Arabidopsis thaliana*. *Proc Natl Acad Sci USA*. 2010; 107: 21199–21204. <https://doi.org/10.1073/pnas.1007431107> PMID: 21078970
3. Lu S, Zhao X, Hu Y, Liu S, Nan H, Li X, et al. Natural variation at the soybean *J* locus improves adaptation to the tropics and enhances yield. *Nat Genet*. 2017; 49: 773–779. <https://doi.org/10.1038/ng.3819> PMID: 28319089
4. Todesco M, Balasubramanian S, Hu TT, Traw MB, Horton M, Epple P, et al. Natural allelic variation underlying a major fitness trade-off in *Arabidopsis thaliana*. *Nature*. 2010; 465: 632–636. <https://doi.org/10.1038/nature09083> PMID: 20520716
5. Chao D-Y, Dilkes B, Luo H, Douglas A, Yakubova E, Lahner B, et al. Polyploids exhibit higher potassium uptake and salinity tolerance in *Arabidopsis*. *Science*. 2013; 341: 658–659. <https://doi.org/10.1126/science.1240561> PMID: 23887874
6. Rubio F, Gassmann W, Schroeder JI. Sodium-driven potassium uptake by the plant potassium transporter *HKT1* and mutations conferring salt tolerance. *Science*. 1995; 270: 1660–1663. PMID: 7502075
7. Uozumi N, Kim EJ, Rubio F, Yamaguchi T, Muto S, Tsuboi A, et al. The *Arabidopsis HKT1* gene homolog mediates inward Na^+ currents in *Xenopus laevis* oocytes and Na^+ uptake in *Saccharomyces cerevisiae*. *Plant Physiol*. 2000; 122: 1249–1259. PMID: 10759522
8. Sunarpi, Horie T, Motoda J, Kubo M, Yang H, Yoda K, et al. Enhanced salt tolerance mediated by *AtHKT1* transporter-induced Na^+ unloading from xylem vessels to xylem parenchyma cells. *Plant J*. 2005; 44: 928–938. <https://doi.org/10.1111/j.1365-313X.2005.02595.x> PMID: 16359386
9. Ren Z-H, Gao J-P, Li L-G, Cai X-L, Huang W, Chao D-Y, et al. A rice quantitative trait locus for salt tolerance encodes a sodium transporter. *Nat Genet*. 2005; 37: 1141–1146. <https://doi.org/10.1038/ng1643> PMID: 16155566
10. Kobayashi NI, Yamaji N, Yamamoto H, Okubo K, Ueno H, Costa A, et al. *OsHKT1;5* mediates Na^+ exclusion in the vasculature to protect leaf blades and reproductive tissues from salt toxicity in rice. *Plant J*. 3rd ed. 2017; 143: 1918. <https://doi.org/10.1111/tbj.13595>
11. DAVENPORT RJ, MUÑOZ-MAYOR A, Jha D, ESSAH PA, Rus A, Tester M. The Na^+ transporter *AtHKT1;1* controls retrieval of Na^+ from the xylem in *Arabidopsis*. *Plant Cell Environ*. 2007; 30: 497–507. <https://doi.org/10.1111/j.1365-3040.2007.01637.x> PMID: 17324235
12. Busoms S, Teres J, Huang X-Y, Bomblies K, Danku J, Douglas A, et al. Salinity Is an Agent of Divergent Selection Driving Local Adaptation of *Arabidopsis* to Coastal Habitats. *Plant Physiol*. 2015; 168: 915–929. <https://doi.org/10.1104/pp.15.00427> PMID: 26034264
13. Rus A, Baxter I, Muthukumar B, Gustin J, Lahner B, Yakubova E, et al. Natural variants of *AtHKT1* enhance Na^+ accumulation in two wild populations of *Arabidopsis*. *PLoS Genet*. 2006; 2: e210. <https://doi.org/10.1371/journal.pgen.0020210> PMID: 17140289
14. Baek D, Jiang J, Chung J-S, Wang B, Chen J, Xin Z, et al. Regulated *AtHKT1* gene expression by a distal enhancer element and DNA methylation in the promoter plays an important role in salt tolerance. *Plant Cell Physiol*. 2011; 52: 149–161. <https://doi.org/10.1093/pcp/pcq182> PMID: 21097475
15. Baxter I, Brazelton JN, Yu D, Huang YS, Lahner B, Yakubova E, et al. A Coastal Cline in Sodium Accumulation in *Arabidopsis thaliana* Is Driven by Natural Variation of the Sodium Transporter *AtHKT1;1*. Copenhaver GP, editor. *PLoS Genet*. 2010; 6: e1001193. <https://doi.org/10.1371/journal.pgen.1001193> PMID: 21085628
16. Berthomieu P, Conéjéro G, Nublát A, Brackenbury WJ, Lambert C, Savio C, et al. Functional analysis of *AtHKT1* in *Arabidopsis* shows that Na^+ recirculation by the phloem is crucial for salt tolerance. *EMBO J*. 2003; 22: 2004–2014. <https://doi.org/10.1093/emboj/cdg207> PMID: 12727868

17. Rus A. *AtHKT1* Facilitates Na⁺ Homeostasis and K⁺ Nutrition in *Planta*. *Plant Physiol.* 2004; 136: 2500–2511. <https://doi.org/10.1104/pp.104.042234> PMID: 15347798
18. Horie T, Horie R, Chan W-Y, Leung H-Y, Schroeder JI. Calcium regulation of sodium hypersensitivities of *sos3* and *athkt1* mutants. *Plant Cell Physiol.* 2006; 47: 622–633. <https://doi.org/10.1093/pcp/pcj029> PMID: 16540484
19. Munns R, Tester M. Mechanisms of salinity tolerance. *Annu Rev Plant Biol.* 2008; 59: 651–681. <https://doi.org/10.1146/annurev.arplant.59.032607.092911> PMID: 18444910
20. Munns R, James RA, Xu B, Athman A, Conn SJ, Jordans C, et al. Wheat grain yield on saline soils is improved by an ancestral Na⁺ transporter gene. *Nat Biotechnol.* 2012; 30: 360–364. <https://doi.org/10.1038/nbt.2120> PMID: 22407351
21. Rodríguez-Rosales MP, Gálvez FJ, Huertas R, Aranda MN, Baghour M, Cagnac O, et al. Plant NHX cation/proton antiporters. *Plant Signal Behav.* 2009; 4: 265–276. PMID: 19794841
22. Feng Z, Zhang B, Ding W, Liu X, Yang D-L, Wei P, et al. Efficient genome editing in plants using a CRISPR/Cas system. *Cell Res.* 2013; 23: 1229–1232. <https://doi.org/10.1038/cr.2013.114> PMID: 23958582
23. Mäser P, Hosoo Y, Goshima S, Horie T, Eckelman B, Yamada K, et al. Glycine residues in potassium channel-like selectivity filters determine potassium selectivity in four-loop-per-subunit HKT transporters from plants. *Proc Natl Acad Sci USA.* 2002; 99: 6428–6433. <https://doi.org/10.1073/pnas.082123799> PMID: 11959905
24. Ali A, Raddatz N, Aman R, Kim S, Park HC, Jan M, et al. A Single Amino-Acid Substitution in the Sodium Transporter HKT1 Associated with Plant Salt Tolerance. *Plant Physiol.* 2016; 171: 2112–2126. <https://doi.org/10.1104/pp.16.00569> PMID: 27208305
25. Oomen RJFJ, Benito B, Sentenac H, Rodríguez-Navarro A, Talón M, Véry A-A, et al. HKT2;2/1, a K⁺-permeable transporter identified in a salt-tolerant rice cultivar through surveys of natural genetic polymorphism. *Plant J.* 2012; 71: 750–762. <https://doi.org/10.1111/j.1365-313X.2012.05031.x> PMID: 22530609
26. Mishra S, Singh B, Panda K, Singh BP, Singh N, Misra P, et al. Association of SNP Haplotypes of HKT Family Genes with Salt Tolerance in Indian Wild Rice Germplasm. *Rice (N Y).* 2016; 9: 15. <https://doi.org/10.1186/s12284-016-0083-8> PMID: 27025598
27. Lin HX, Zhu MZ, Yano M, Gao JP, Liang ZW, Su WA, et al. QTLs for Na⁺ and K⁺ uptake of the shoots and roots controlling rice salt tolerance. *Theor Appl Genet.* 2004; 108: 253–260. <https://doi.org/10.1007/s00122-003-1421-y> PMID: 14513218
28. Genc Y, McDonald GK, Tester M. Reassessment of tissue Na⁽⁺⁾ concentration as a criterion for salinity tolerance in bread wheat. *Plant Cell Environ.* 2007; 30: 1486–1498. <https://doi.org/10.1111/j.1365-3040.2007.01726.x> PMID: 17897418
29. Jaime-Pérez N, Pineda B, García-Sogo B, Atares A, Athman A, Byrt CS, et al. The sodium transporter encoded by the HKT1;2 gene modulates sodium/potassium homeostasis in tomato shoots under salinity. *Plant Cell Environ.* 2017; 40: 658–671. <https://doi.org/10.1111/pce.12883> PMID: 27987209
30. Cuartero J, Bolarín MC, Asíns MJ, Moreno V. Increasing salt tolerance in the tomato. *J Exp Bot.* 2006; 57: 1045–1058. <https://doi.org/10.1093/jxb/erj102> PMID: 16520333
31. Mäser P, Eckelman B, Vaidyanathan R, Horie T, Fairbairn DJ, Kubo M, et al. Altered shoot/root Na⁺ distribution and bifurcating salt sensitivity in *Arabidopsis* by genetic disruption of the Na⁺ transporter *AtHKT1*. *FEBS Lett.* 2002; 531: 157–161. PMID: 12417304
32. Mao J, Zhang Y-C, Sang Y, Li Q-H, Yang H-Q. From The Cover: A role for *Arabidopsis* cryptochromes and COP1 in the regulation of stomatal opening. *Proc Natl Acad Sci USA.* 2005; 102: 12270–12275. <https://doi.org/10.1073/pnas.0501011102> PMID: 16093319
33. Chao D-Y, Chen Y, Chen J, Shi S, Chen Z, Wang C, et al. Genome-wide association mapping identifies a new arsenate reductase enzyme critical for limiting arsenic accumulation in plants. Maloof JN, editor. *PLoS Biol.* 2014; 12: e1002009. <https://doi.org/10.1371/journal.pbio.1002009> PMID: 25464340
34. Livak KJ, Schmittgen TD. Analysis of Relative Gene Expression Data Using Real-Time Quantitative PCR and the 2^{-ΔΔCT} Method. *Methods.* 2001; 25: 402–408. <https://doi.org/10.1006/meth.2001.1262> PMID: 11846609